Detection of Intracochlear Damage During Cochlear Implant Electrode Insertion using Extracochlear Measurements in the Gerbil

Faisal I. Ahmad, BS, **Baishakhi Choudhury, MD**, **Christine E. DeMason, BS**, **Oliver F. Adunka, MD**, **Charles C. Finley, PhD**, and **Douglas C. Fitzpatrick, PhD**
Department of Otolargynology/Head and Neck Surgery, University of North Carolina at Chapel Hill, Chapel Hill, NC, USA

Abstract

Objectives—An intraoperative monitoring algorithm during cochlear implant electrode insertion could be used to detect trauma and guide electrode placement relative to surviving hair cells. The aim of this report was to assess the feasibility of using extracochlear recording sites to monitor acoustically evoked responses from surviving hair cells and neural elements during implantation in an animal model.

Design—The normal-hearing gerbil was used. Two recording methods, one using a lock in amplifier and another using Fourier analysis of recorded signals were used to obtain frequency specific information about the responses to tones. Amplitude and threshold determinations were made at the round window and at three extracochlear sites. To induce intracochlear damage, a platinum-iridium wire was inserted through the round window. The wire was advanced and changes in the potentials were correlated with cochlear contact. Anatomical integrity was assessed using cochlea whole mount preparations.

Results—In general, the lock-in amplifier showed greater sensitivity and lower thresholds at higher frequencies relative to the Fourier method. Also, the lock-in amplifier was more resistant to masking effects. Both systems were able to detect loss of cochlear potentials secondary to intracochlear trauma. Histological damage was seen in all cases and corresponded to electrophysiological changes.

Conclusions—Impact of electrodes on cochlear structures affecting cochlear performance could be detected from several extracochlear sites. The lock-in amplifier demonstrated greater sensitivity and resistance to noise when compared to the FFT recording paradigm. The latter showed greater flexibility of detecting and separating hair cell and neural potentials.

Correspondence: Oliver F. Adunka, MD, Assistant Professor, Otology, Neurotology, Skull Base Surgery, Department of Otolaryngology/Head and Neck Surgery, University of North Carolina at Chapel Hill, POB, 170 Manning Drive, CB# 7070, Chapel Hill, NC 27599-7070, Phone: (919) 966-3342, Fax: (919) 966-7656, adunka@med.unc.edu.

Conflict of Interest: none

INTRODUCTION

With the development of combined electric and acoustic stimulation (EAS), preservation of residual hearing has become an important consideration during cochlear implantation. The main benefit of EAS is improved speech discrimination in noise[1–4]. Despite multiple efforts to enhance the likelihood to preserve residual hearing, a substantial degree of hearing is lost as a result of cochlear implantation in approximately 50% of patients[4,5]. Such efforts include less traumatic electrode insertions to preserve the anatomical and functional integrity of the cochlea. However, intracochlear trauma may contribute to decreased implant performance in patients where electrodes are dislocated into the scala vestibuli[6,7]. Thus, cochlear implant patients can benefit from non-traumatic electrode placements, regardless of the status of residual hearing.

We are presently using an animal model to develop an intraoperative monitoring system with the goal to provide real-time information about cochlear functional status during the electrode insertion process. In the gerbil, we have demonstrated that reductions in intracochlear potentials, specifically the cochlear microphonic (CM) and compound action potential (CAP), provide information about the interaction of the electrode with cochlear structures[8–10]. Upon contact with the basilar membrane or osseous spiral lamina, reductions in the CM and CAP occur across a wide range of frequencies and intensities[9]. Consequently, a reduced stimulus set consisting of one tonal frequency and intensity combination can be used to detect reversible physiologic changes[8]. These experiments suggest that an efficient paradigm of cochlear monitoring suitable for intraoperative use can be developed.

All of our previous experiments have simulated a recording site from the electrode itself as it advances. Though intracochlear electrophysiological recordings are a logical application of the current technical capabilities, this method has some limitations. For example, intracochlear recordings must be measured through the back-telemetry hardware and software provided by the implant manufacturers, which is not optimized for recording potentials evoked by acoustic stimulation. Another significant limitation relates to the spatial distance of the implant from hair cells; in particular, measured amplitudes are a function of both this distance and the status of the hair cells themselves. As such, this confounding factor makes it difficult to determine whether amplitude reductions are due to impaired hair cell function or due to a greater distance between the recording electrode and the hair cells.

An alternative approach for monitoring hair cell status is to record from a single stationary, extracochlear site during insertion. Here, we explore the use of two extracochlear recording systems to overcome dependence of signal strength on the distance from the recording electrode, thus better reflecting the status of the cochlea as the electrode advances. However, because an extracochlear electrode is on bone instead of in fluid, there is diminished signal quality so that more averaging and time may be needed to obtain measurements. In our previous studies, we used traditional amplifiers, and the fast Fourier transform (FFT) algorithm for signal processing and analysis[8–11]. In this experiment we compare this strategy with an alternative, which is to use a lock-in amplifier. The lock-in amplifier has traditionally been found advantageous in conditions that required recovering signals at low signal-to-noise ratios[12], and has been used previously in auditory research because of these strengths[13]. This amplifier provides an output that is proportional to signals components that are synchronous with a standard reference frequency. This strategy can offer better signal detection and noise reduction/rejection, potentially allowing recordings to be made with minimal averaging to overcome the diminished signal quality.

MATERIALS AND METHODS

Results from 15 Mongolian gerbils (*Meriones unguiculatus*) are reported. The gerbil was chosen because of its sensitive low frequency hearing and easily accessible cochlea. All animals were handled and housed according to the standards described by the National Institutes of Health Committee on Care and Use of Laboratory Animals, using protocols approved by the Institutional Animal Care and Use Committee (IACUC).

Animal Handling

Surgeries and recordings were performed under deep urethane anesthesia (25% solution in saline, 1.5 g/kg, i.p.). Once anesthesia was induced, the animal was moved to a double-walled, sound attenuated booth. The core body temperature was monitored with a rectal probe and maintained around 37°C with heating pads and an incandescent heat lamp.

Surgical Procedure

The bony bulla was exposed and opened with a standard postauricular skin incision and the pinna was removed. The recording electrode, which was attached to a micromanipulator, was placed adjacent to the intact round window membrane or one of four extracochlear sites, the round window (RW), the basal cochlea (between the round and oval windows), the promontory, or the stapes footplate.

Electrode & Recording Configuration

For measurements at the round window, the electrode was a Teflon-insulated, tungsten-iridium wire 50 μm in diameter with approximately 50 μm of tip insulation removed. For recordings on bony sites, the recording electrode was a 180 μm diameter, Teflon-insulated rigid silver wire with approximately 1-mm of tip insulation removed. In both cases, the recording was differential and monopolar, with the electrode connected to the positive input of a preamplifier (Grass Instruments, model P15D, West Warwick, RI, USA). A wire clipped to the neck musculature was the negative input and the system ground was the animal's tail. The preamplifier provided 100-fold amplification with bandpass filters at 10 Hz and 50 kHz. The signal was then sent to one of two additional amplifiers depending on the processing method (FFT or lock-in hardware).

Recordings using with the fast Fourier transform (FFT) method (see below) underwent additional amplification (10×) and filtering (10 – 100,000 Hz) with an EG&G Instruments amplifier (model 5113 Albuquerque, NM, USA). The waveform was then digitized (200 kHz sampling rate) and 100 stimulus repetitions were averaged.

Recordings with the lock-in amplifier underwent 10× amplification through a Stanford Research Systems (SRS) lock-in preamplifier (model SR550, Sunnyvale, CA, USA); and subsequently the signal was presented to the SRS lock-in amplifier (model SR 830). The sync output (5 V square wave at the stimulus frequency) of the function generator was used as the reference signal for the lock-in amplifier. The sensitivity of the lock-in was adjusted from 20 μV to 1 V for a full 5 V output depending on the magnitude of the incoming signal. The dynamic reserve was set to the normal setting and a 24 dB/octave filter was selected. A time constant of 1 second was chosen. A 5 s epoch of the waveform was digitized (2 kHz sampling rate) and recorded after it had reached steady-state (see Fig. 1D).

Acoustic Stimulation & Calibration

Different acoustic stimuli were used for each recording and analysis method. For FFT analyses the stimuli were short tone bursts consisting of a 10 ms plateau with 2 ms rise/fall times presented with a 30 ms interstimulus interval. The tone bursts were produced using

custom software and a National Instruments input/output board (Model 6250E, Austin, TX, USA). For the lock-in amplifier, continuous tones were used. These were produced with a Hewlett-Packard function generator (33120A, Palo Alto, CA, USA) and Tucker-Davis programmable attenuator (PA5, Alachua, FL, USA). With both methods the generated electrical signals were delivered through a Tucker-Davis system III headphone buffer (model HB7) to a well-shielded loudspeaker (Beyerdynamic DT-48, Farmingdale, NY, USA). Calibration was performed using a ¼" Bruel and Kjaer microphone (Nærum, Denmark) placed at the position of the animal's eardrum and levels were presented in dB sound pressure level (SPL, re 20 μPa).

Masked thresholds

The ability of the FFT analysis and lock-in amplifier to detect signals in the presence of a masker signal was compared. The acoustic masker consisted of broadband noise (10 Hz to 32 kHz) that was constructed with custom software and presented through a separate speaker (Morel ET-338, Ness Ziona, Israel). Calibration was performed once, using a ¼" Bruel and Kjaer microphone placed at the position of an animal's eardrum. Performance of both recording paradigms in the presence of an electrical masker was also assessed. The electrical masker consisted of 60 Hz alternating current (AC) noise obtained by unshielding a standard wall outlet, which results in approximately 100 mV in amplitude at the recording electrode.

Intracochlear damage

A rigid Teflon insulated wire as detailed above was attached to a hydraulic micromanipulator, which was controlled from outside of the sound booth, was used to produce intracochlear damage. Initially the wire was placed against the intact round window membrane and subsequent penetrations were made into the scala tympani. Penetration trajectories were radial through the scala tympanic, i.e., roughly perpendicular to the long axis and aimed at the basilar membrane. From the extracochlear sites, recordings of the cochlear potentials to acoustic stimuli were made at 200 μm intervals as the electrode was advanced. Stimuli for the FFT and lock-in amplifier analyses were 4 kHz tones (see above) presented at 70 dB SPL.

After each experiment both cochleae we fixed and removed en block. Cochleae were decalcified, prepared as a whole mount and stained with toluidine blue. Cochlear damage due to the electrode was photographed at 10–50× with a Wild M50 dissecting microscope (Leica Inc., Wetzlar, Germany).

Data collection and analysis

For the FFT analysis, the cochlear microphonic (CM) and compound action potential (CAP) were separated by filtering and analyzing particular epochs of the recorded waveform (see Fig. 1B and C). The CAP was complete after the first ms of the response while the CM was present throughout the stimulus. The FFT analysis was from the last 5 ms of the 10 ms plateau, i.e., remote from the CAP. The magnitude of response at the stimulus frequency was determined from the amplitude component of the FFT. The noise floor for each recording was measured by analyzing the response in the last 5 ms of the interstimulus period.

The lock-in amplifier produced a direct current (DC) output that was proportional to the magnitude of the cochlear response at the reference frequency. To allow the output time to rise to its final value, the cochlear response was calculated by the steady-state values obtained after five time-constants were allowed to pass. The noise floor was determined by measuring response to a no-stimulus condition.

RESULTS

A single recording obtained with each method is shown in Figure 1: a recording to a tone-burst is displayed in Figure 1A. This cochlear response is a summation of the CAP and CM. Filtering from 500 – 1500 Hz removed the CM component and left the neural component or CAP (Fig. 1B). Performing an FFT of the raw waveform (window 6–11 ms to avoid the CAP) produced a frequency domain plot (Fig. 1C) with a peak at the stimulus frequency. The magnitude of the CM was taken as this peak measurement. Figure 1D displays cochlear response to a continuous tone after lock-in amplifier processing. The output of the lock-in amplifier was a DC signal whose magnitude is proportional to the magnitude of the signal at the reference frequency. In Figure 1D, time zero corresponds to the onset of the recording epoch. There was a significant delay, corresponding to about five time constants before the signal reached steady-state.

Because the lock-in measurement is based on a continuous tone there is no CAP produced. Consequently, all subsequent comparisons using the tone bursts are with the FFT results (as in Fig. 2C).

Growth Functions

Growth functions (level series) were obtained at six frequencies (500–16000 Hz in one-octave steps) starting at the round window and then at the three other extracochlear sites, using both the FFT system and lock-in amplifier. The maximum range of intensities was between –17 and 95 dB SPL depending on the frequency. Representative growth functions for the FFT (left panels) and lock-in (right panels) at one- and eight-kilohertz (top and bottom panels, respectively) are displayed in Figure 2. The growth functions at 1 kHz showed significant non-linearity at suprathreshold levels using both recording methods. In particular, a prominent decrease in response was noted at 58 dB (arrows). Non-linearities were typical of growth functions performed at frequencies below 2 kHz.

For the FFT analysis, the noise floor (dotted line) was calculated as the response in the last 5 ms of the interstimulus interval, and then averaged across intensities. For the lock-in analysis, the speaker output was disconnected and three recordings of these no-stimulus conditions were taken. The average response was calculated and used as the noise floor. The threshold determinations (arrowheads) for the FFT and lock-in at 1 kHz (panels A and C) were 39 and 29 dB SPL, respectively. With the 8 kHz stimulus (Fig. 2, panel B and D), thresholds were 27 and 7 dB SPL for FFT and lock-in amplifier, respectively.

Threshold determinations were made at the RW in nine animals (Figure 3). Lock-in measurements achieved lower thresholds for all frequencies except 0.5 kHz, though measurements were only statistically different (asterisks) for 4, 8, and 16 kHz (paired t-tests, p<0.01). Both the FFT and lock-in analysis achieved the lowest thresholds at 8 kHz.

Masked RW responses

In order to compare the lock-in amplifier to our traditional FFT-based system in the setting of low signal-to-noise ratios, we examined both systems' ability to detect cochlear signals in the presence of both an acoustic and electrical masker. The acoustic masker consisted of band-pass noise between 10 Hz and 32 kHz, calibrated for the speakers output. Figure 4 displays cochlear response to a 75 dB SPL stimulus in the presence of 20, 40, and 60 dB SPL of acoustic noise. The magnitudes of the masked cochlear responses were normalized relative to the unmasked condition (Fig. 4A). For both measures the response was reduced by an amount proportional to the masker level. The lock-in amplifier was less affected by the masking than was the FFT method. Threshold measurements followed a similar pattern,

with increases proportional to masker intensity for both methods, but the lock-in amplifier showed smaller increases than the FFT method.

The performance of both recording paradigms was also assessed in the presence of an electrical masker, which consisted of 60 Hz AC noise, 100 mV in magnitude. The FFT system showed a 34% decline in response to a 4 kHz stimulus at 75 dB SPL, while the lock-in amplifier demonstrated a 26% decline. Thresholds at 4 kHz were relatively resistant to the electrical noise, with a 4 dB increase for the FFT method and 12 dB for the lock-in amplifier.

Extracochlear detection of intracochlear trauma

Three extracochlear sites (Fig. 5) were examined. The stapes footplate (Fig. 5A) overlies the oval window. The cochlear base (Fig. 5D) is the bony surface between the round and oval windows. The promontory (Fig. 5G), is part of the bony canal of the first cochlear turn. Threshold determinations were made at each extracochlear site (Figs. 5B, E, and H). As with recordings at RW (Fig. 3), the lock-in amplifier produced better thresholds at most frequencies, particularly higher frequencies.

After threshold determinations were made, the penetrating wire was placed at the RW membrane and inserted towards the basilar membrane. Baseline measurements at the RW served as the "standard", and responses taken with electrode advancement were compared to this standard (Figs. 5C, F, and I). In all three cases, abrupt declines in intracochlear potentials were detectable from the extracochlear sites, indicative of cochlear damage (arrows). In two of the cases (Figs 5C and I), an abrupt decline was noted with advancement. In the third case (Fig. 5F), a progressive decline was noted followed by a more precipitous decline. In all cases, the electrode was either partially or fully withdrawn to the starting position at the RW (break in the depth axis in each panel). The potentials either declined further or remained stable, indicating non-reversible damage.

Subsequently, cochleae from these cases were prepared for morphological assessment. A representative example (Fig. 6) was taken from a recording with the electrode at the stapes footplate. Damage (within the box) consisted of a clear breach of the basilar membrane. The position of this damage correlated with the depth where the physiological response showed a sharp drop (between 800–1000 um, Fig. 5C). A similar correlation was seen in all other cases as well, indicating that the sharp drops in measured potentials correspond to damage of cochlear structures due to electrode impact.

DISCUSSION

Both, the FFT-based recording paradigm and the lock-in amplifier technology were able to detect cochlear trauma during cochlear implantation. The lock-in amplifier provided better sensitivity at some frequencies and slightly better noise rejection. In the following, we will discuss the strengths and weaknesses of each method for the purpose of recording during cochlear implantation.

Growth functions at the RW

Using both the FFT and lock-in methods, the growth functions for tone frequencies of 4 kHz and above displayed a linear relationship between stimulus intensity and cochlear response at suprathreshold levels, while frequencies of 0.5–2 kHz demonstrated significant growth function non-linearities (Fig. 2). These were previously observed in the gerbil and were assumed to be due to interaction of the CM with a phase-locked neural component. In the gerbil, recordings in cochlear nerve fibers show phase-locking to be maximal at 500 Hz and insignificant above 4 kHz[14], which correlates well with the linear CM functions seen here at

4 kHz and above. The evoked potential correlate of phase-locking is the neurophonic (N), previously shown in the gerbil to be a prominent part of the response to low frequency tones recorded at the RW[15]. Thus, for low frequencies the FFT detects "CM+N", rather than CM alone. The neurophonic is ½-wave rectified and delayed relative to the CM. These factors, coupled with any differences in the growth curve of the sources, result in a complex interaction between the neurophonic and CM and a non-linear growth function for the combined signals. Henry et al[15] demonstrated that suppression of the neural component with tetrodotoxin re-established a linear relationship between stimulus intensity and the CM.

The lowest thresholds overall were obtained using the lock-in amplifier at higher frequencies. From 4–16 kHz, the lock-in produced average thresholds that were 13–23 dB lower than with the FFT method in nine animals (Fig. 3). Lock-in performance was also slightly better than the FFT at 1 and 2 kHz (6 dB each) but the differences were not significant. It is not entirely clear why the comparison shows this difference across frequency, because neither method has a frequency limitation within the range studied. The differences scale roughly both with background noise and overall signal strength. The noise levels show the expected 1/f decline in physiological signals. The signal strength across frequency is related to the position of the recording electrode relative to the tonotopic organization of the cochlea. With our monopolar recordings, 4 and 8 kHz showed the strongest signals. The regions corresponding to the characteristic frequencies of 0.5–2 kHz are located more apically, and the signals at the RW are proportionally smaller. However, these differences should be detected in a similar fashion by both measures. A possible reason for the difference between methods is the acoustic signal used, which was a tone burst for the FFT and a continuous tone for the lock-in amplifier. With the tone bursts, the large CAP has a frequency content that spans the low frequency range of 0.5–2 kHz. Although we largely excluded the CAP by windowing the signal for FFT analysis from 6–11 ms (Fig. 1B and C), it is possible that some of this signal intruded on the FFT measurements. We think the most likely reason for the difference is due to the neurophonic, which is lacking at higher frequencies. The broader spectral width may include more energy from this ½ rectified version of the stimulus frequency than is the case with the lock-in amplifier, although both show the effect of the interaction.

Noise rejection with the two methods

The intraoperative environment is subject to significant acoustic and electric background noise. Consequently, we sought to compare the FFT and lock-in amplifier with regards to their ability to make measurements in the presence of maskers. In the presence of a 20 dB noise masker the FFT method showed a moderately large decrement in sensitivity, and subsequently showed a more incremental decrease in the presence of louder maskers. Averaging over 100 trials was used with the FFT method to improve the signal-to-noise level, which could be further improved with more averaging. In contrast, the lock-in amplifier showed modest decrease in signal in the presence of the 20 and 40 dB maskers, and then showed a larger decrease with the loudest masker. The lock-in amplifier's noise rejecting capabilities are based on employment of phase- and frequency-dependent signal detection and time-constant selection. The lock-in essentially functions as a bandpass filter and the time-constant (T) determines its effective bandwidth defined by the following relationship: bandwidth = 1/4T. Thus, the lock-in amplifiers noise-rejecting ability can be improved by selection of a longer time constant but this results in longer time required for signal acquisition.

Extracochlear Recordings

In cases using a separate cochleostomy, the RW should be an excellent recording site. However, this location may not be practical for procedures involving prospective EAS

patients where the insertion is through the RW. Consequently, additional extracochlear sites further from the RW were examined. In the three additional locations tested (stapes footplate, cochlear base and cochlear promontory) the lock-in amplifier provided overall lower thresholds, similar to the results at the RW. These results support the view that the lock-in amplifier has the potential to obtaining either equivalent or more sensitive thresholds than the FFT method at a given site, depending on frequency examined.

Overall, threshold measurements made at extracochlear locations were higher than their counterparts at the RW. For RW recordings, we placed our recording electrode in fluid that is typically present in the RW niche. The RW membrane is semi-permeable and is therefore functionally continuous with the perilymph of the scala tympani, making it a well-suited recording site for sensitive measurements. At all other extracochlear sites the recording electrode was placed on bone, which would not be as conductive of intracochlear potentials. Although recording at the stapes footplate has the advantage of being close to the oval window, the electrode at this location still resides on bone and may be in fact hindering the movement of the footplate and affecting transmission of acoustic energy to the cochlea.

At each of these sites, both the FFT and lock-in systems could detect cochlear trauma using a single frequency (4 kHz) at a high intensity (75 dB SPL). The ability to detect damage with a limited stimulus set is critical to the design of an intraoperative recording system. We have previously shown that a breach of the basilar membrane causes response reductions across a wide range of stimulus frequencies and intensities so a limited stimulus set is feasible[9]. We have also demonstrated that changes with the same stimulus used here for the FFT method (4 kHz tone bursts at suprathreshold intensity) can detect decrements in response that are small enough to be reversible upon electrode retraction. We did not attempt similar measures here as the use of the two methods was too time consuming to permit small steps of advancement. However, it is clear that either method is capable of detecting changes in response magnitude of similar size.

CONCLUSIONS

While both methods show promise for recording during a human cochlear implantation, there are trade-offs with each. With the lock-in amplifier, thresholds at most frequencies were lower and the ability to reject acoustic noise was higher than with the FFT method. Thus, the lock-in amplifier would be superior in applications where the signals to be detected are small and extraneous noise levels are high. This indication is not quite as strong as expected, because at low frequencies the thresholds with the two methods were comparable. The advantage of the FFT is flexibility in terms of detecting and measuring signals generated in the cochlea. The FFT method identifies the CAP (neural component at stimulus onset), the CM to high frequencies or the CM+N to low frequencies. By inverting the phase of low frequency tones the FFT can reduce the CM to isolate the neural component. In contrast, the lock-in provides a DC output proportional to the synchronous input of a reference frequency, and thus is a single value. The continuous acoustic stimulus means that there is no CAP. Alternation is not available, so there is little ability to isolate the neurophonic. For these reasons, we think the FFT provides a greater amount of information about hair cell and neural health during the implantation. However, the greater sensitivity of the lock-in amplifier may be a useful adjunct in some cases.

Acknowledgments

REFERENCES

1. von Ilberg CA, Baumann U, Kiefer J, Tillein J, Adunka OF. Electric-acoustic stimulation of the auditory system: a review of the first decade. Audiol Neurootol. 2011; 16(Suppl 2):1–30. [PubMed: 21606646]

2. Kang SY, Colesa DJ, Swiderski DL, Su GL, Raphael Y, Pfingst BE. Effects of hearing preservation on psychophysical responses to cochlear implant stimulation. J Assoc Res Otolaryngol. 2010; 11:245–265. [PubMed: 19902297]

3. Gantz BJ, Turner C, Gfeller KE, Lowder MW. Preservation of hearing in cochlear implant surgery: advantages of combined electrical and acoustical speech processing. Laryngoscope. 2005; 115:796–802. [PubMed: 15867642]

4. Gstoettner WK, Van De Heyning P, O'Connor AF, et al. Electric acoustic stimulation of the auditory system: results of a multi-centre investigation. Acta Otolaryngol. 2008:1–8.

5. Fraysse B, Macias AR, Sterkers O, et al. Residual hearing conservation and electroacoustic stimulation with the nucleus 24 contour advance cochlear implant. Otol Neurotol. 2006; 27:624–633. [PubMed: 16868510]

6. Skinner MW, Holden TA, Whiting BR, et al. In vivo estimates of the position of advanced bionics electrode arrays in the human cochlea. Ann Otol Rhinol Laryngol Suppl. 2007; 197:2–24. [PubMed: 17542465]

7. Aschendorff A, Kromeier J, Klenzner T, Laszig R. Quality control after insertion of the nucleus contour and contour advance electrode in adults. Ear Hear. 2007; 28:75S–79S. [PubMed: 17496653]

8. Campbell AP, Suberman TA, Buchman CA, Fitzpatrick DC, Adunka OF. Correlation of early auditory potentials and intracochlear electrode insertion properties: an animal model featuring near real-time monitoring. Otol Neurotol. 2010; 31:1391–1398. [PubMed: 20856155]

9. Adunka OF, Mlot S, Suberman TA, et al. Intracochlear recordings of electrophysiological parameters indicating cochlear damage. Otol Neurotol. 2010; 31:1233–1241. [PubMed: 20818290]

10. Campbell AP, Suberman TA, Buchman CA, Fitzpatrick DC, Adunka OF. Flexible cochlear microendoscopy in the gerbil. Laryngoscope. 2010; 120:1619–1624. [PubMed: 20564668]

11. Suberman T, Campbell A, Adunka O, Buchman C, Roche J, Fitzpatrick D. A gerbil model of sloping sensorineural hearing loss. Otol Neurotol. 2011 In Press.

12. Simpson, RE. Introductory electronics for scientists and engineers. Boston: Allyn and Bacon; 1974.

13. Fitzgerald JJ, Robertson D, Johnstone BM. Effects of intra-cochlear perfusion of salicylates on cochlear microphonic and other auditory responses in the guinea pig. Hear Res. 1993; 67:147–156. [PubMed: 8340266]

14. Versteegh CP, Meenderink SW, van der Heijden M. Response Characteristics in the Apex of the Gerbil Cochlea Studied Through Auditory Nerve Recordings. J Assoc Res Otolaryngol. 2011

15. Henry KR. Auditory nerve neurophonic recorded from the round window of the Mongolian gerbil. Hear Res. 1995; 90:176–184. [PubMed: 8974995]
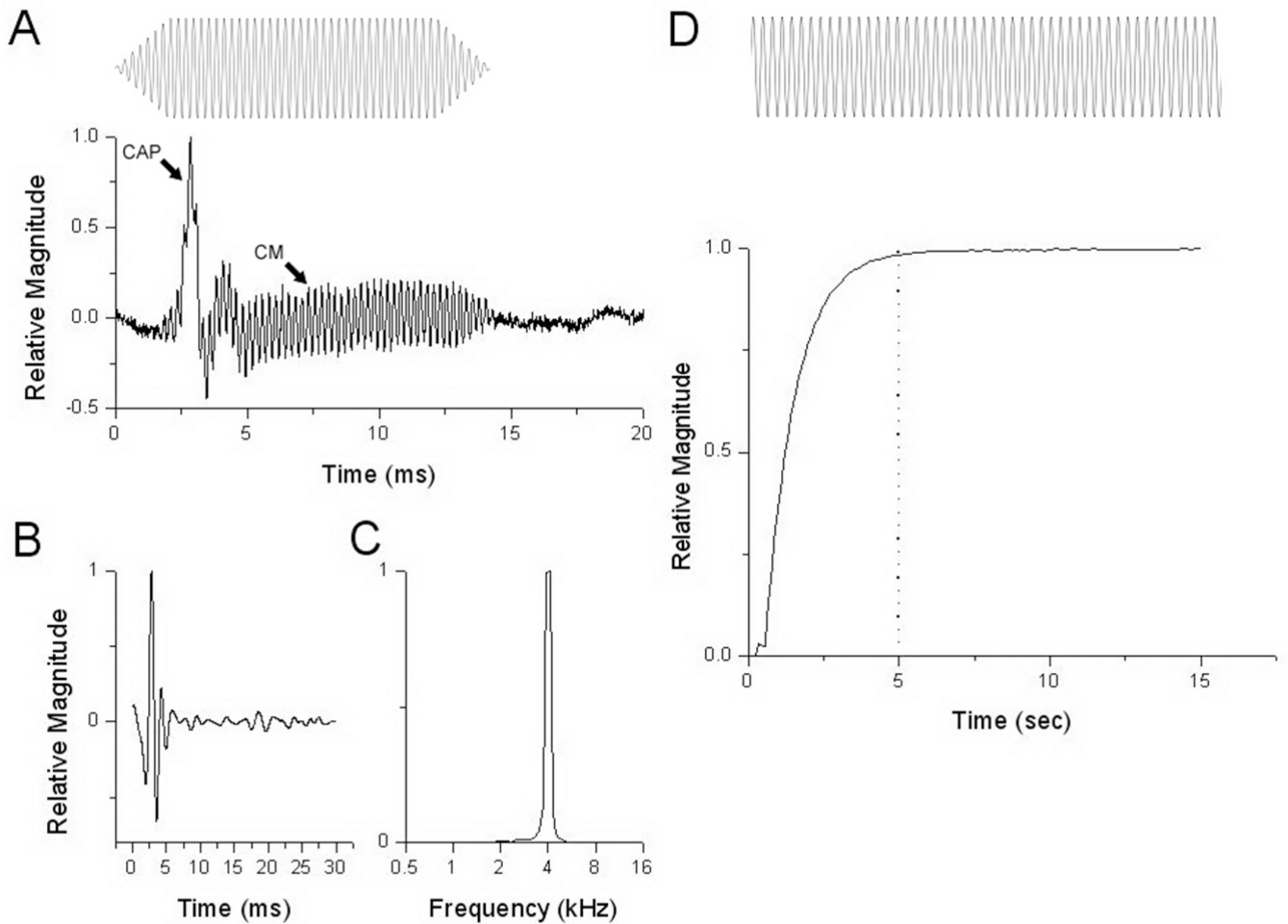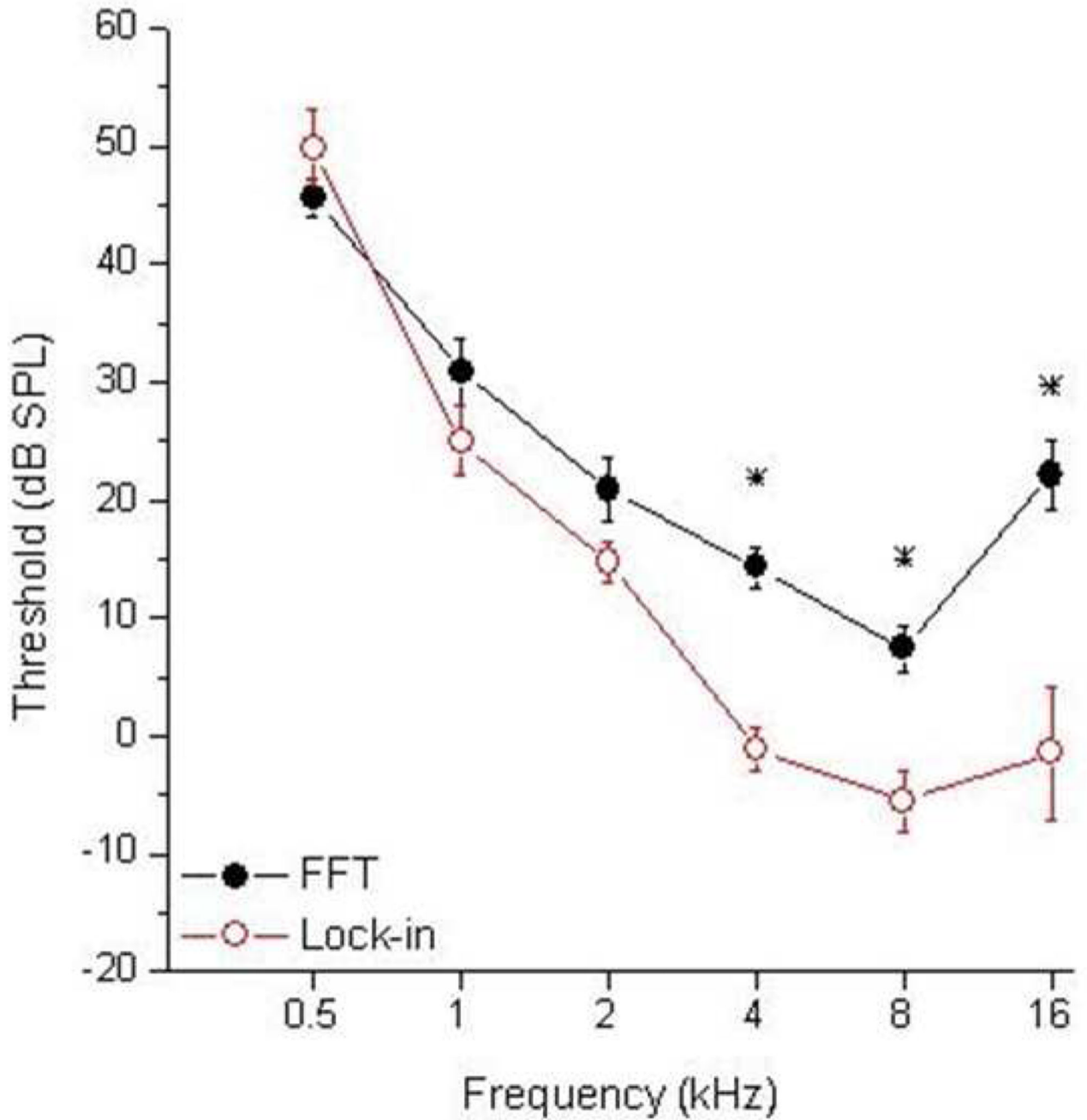
Figure 1.
Acoustic stimulus and measured responses for the Fourier analysis (A–C) and lock-in amplifier (D). Signals in A–D are normalized to the maximum response for each. **A**: The stimulus for the FFT analysis was a tone-burst with 2-ms rise, 10-ms plateau, and a 2-ms fall (schematic at top). The raw recording to a 4 kHz stimulus at 70 dB SPL (bottom) showed an early peak corresponding to the CAP and an ongoing sinusoidal response corresponding to the CM. **B**: The raw recording was filtered from 0.5 to 1.5 kHz to isolate the CAP. **C**: The power spectrum of the CM, taken from an epoch (7–12 ms) uncontaminated by the CAP. **D**: The stimulus for the lock-in amplifier (top) was a continuous tone. The response to a 4 kHz acoustic stimulus at 70 dB SPL (bottom) is a DC output proportional to the signal strength at a known reference frequency, which was obtained from the sync output of the signal generator used to produce the stimulus. Time zero corresponds to onset of the stimulus. The dotted line indicates 5 time constants, or the time required for the output to reach a steady state value. Measured values of cochlear response were obtained by averaging a five second epoch after at least 5 time constants had passed.
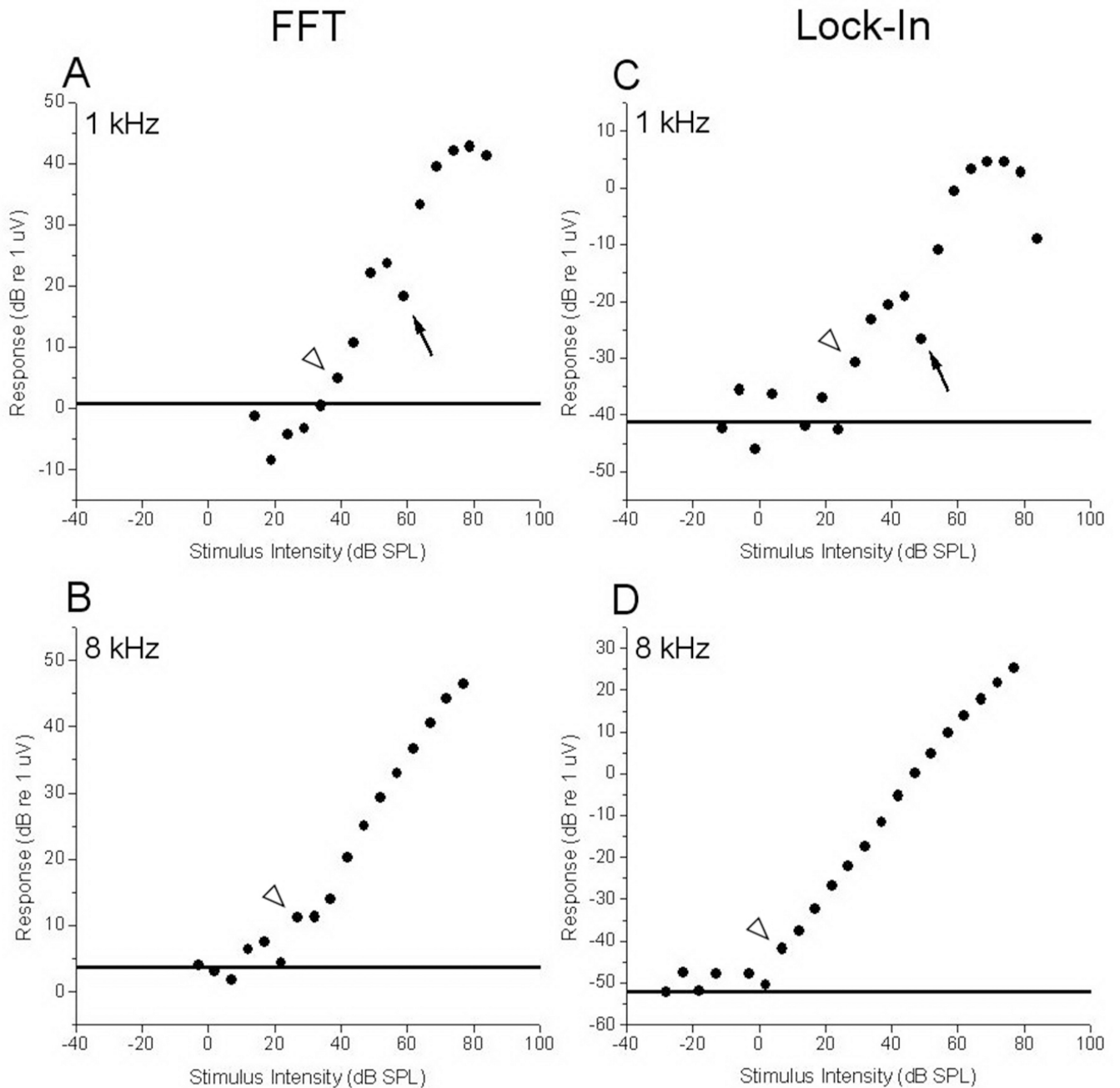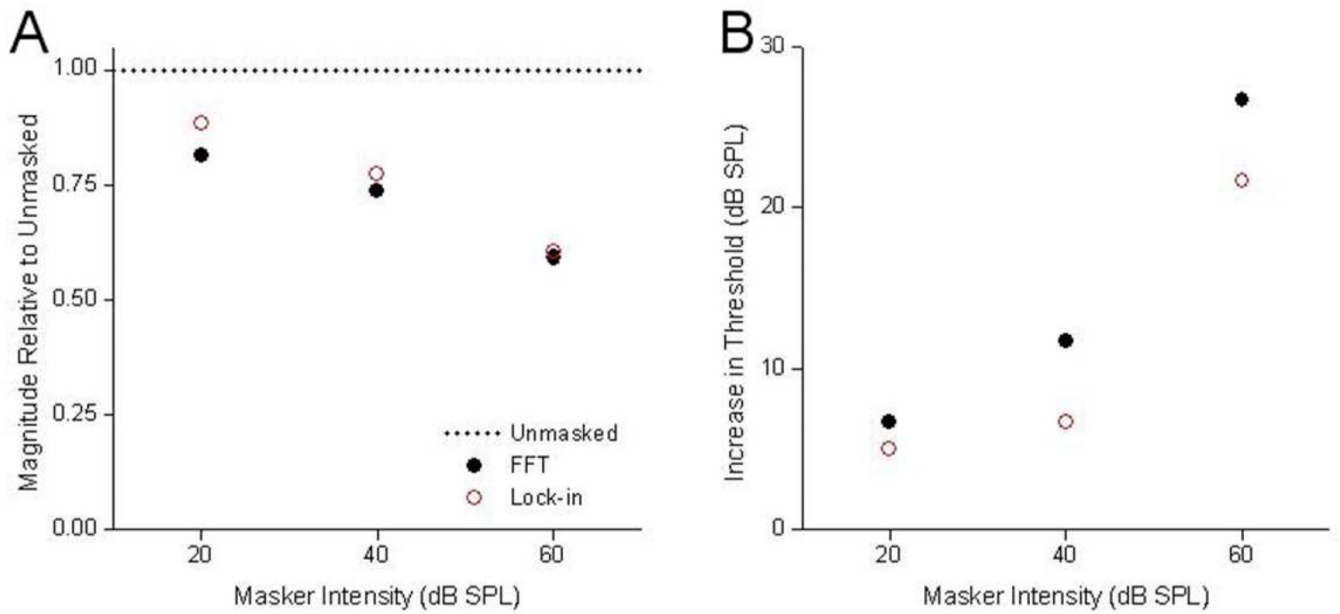
Figure 2.
Growth functions at 1- and 8-kHz as determined by the FFT method (left panels) and lock-in amplifier (right panels) for a representative case. Thresholds are indicated by arrowheads. Solid lines indicate the noise floor. **A & C**: Growth functions to 1-kHz tones. At this frequency both recording methods showed significant non-linearity in the response with a dip in response at 59 dB (arrows). **B & D**: Growth functions to 8 kHz tones. At this frequency, both methods showed a monotonic response increase with increased stimulus intensity.
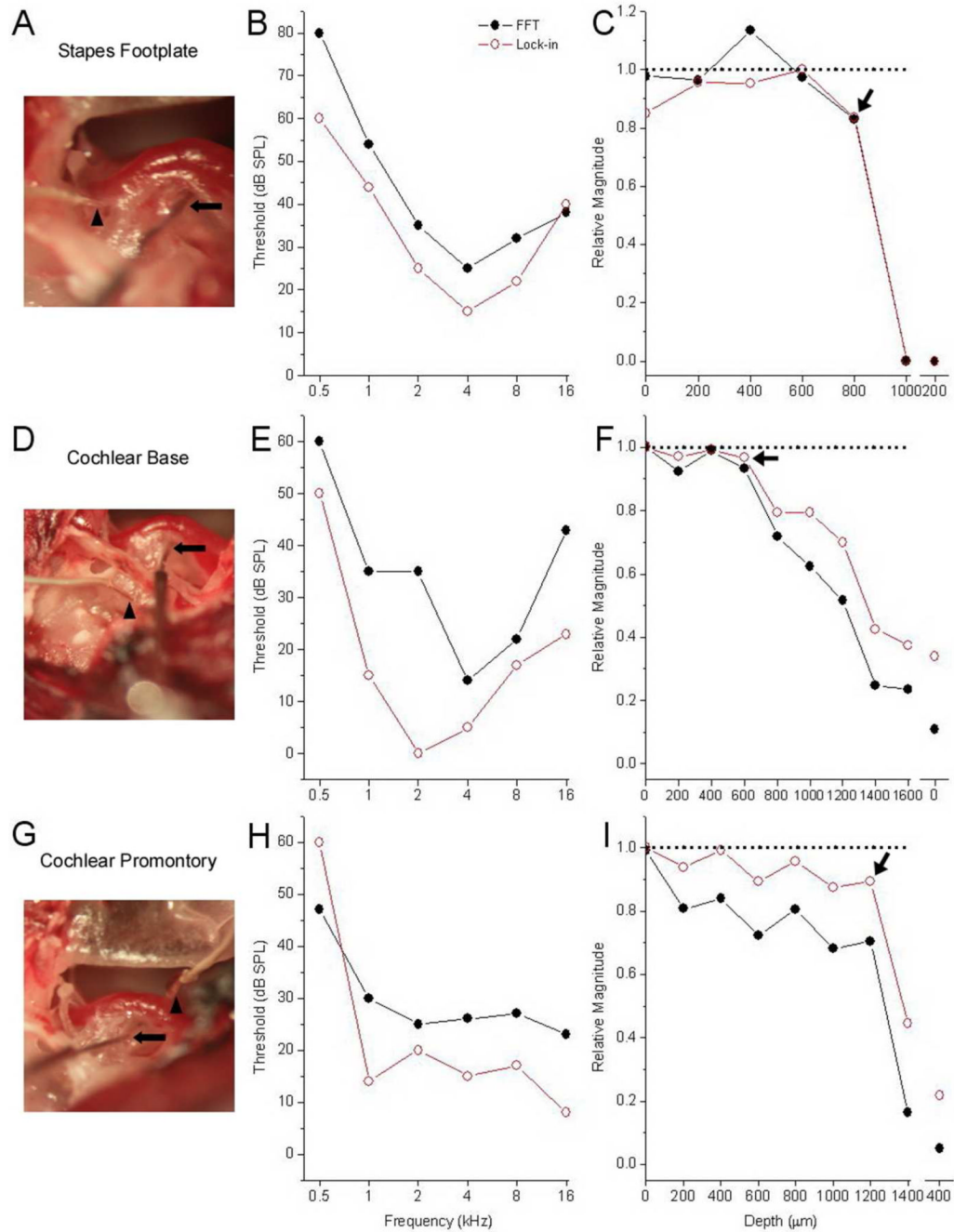
Figure 3.
Comparison of RW thresholds (dB SPL) between the FFT system (black) and the lock-in amplifier (red) at 0.5, 1, 2, 4, 8, and 16 kHz. Plotted data is an average of nine gerbils and error bars indicate standard error.

Figure 4.
Results with an acoustic masker. The masker was noise that was band-passed between 10 Hz
and 32 kHz. The results shown are the average of three animals. **A**: Changes in response
magnitude. The responses were to a 75 dB, 4 kHz tone in the presence of varying intensities
of a masker. The responses are shown relative to those in the unmasked condition (dotted
line). The lock-in response was less affected by the noise than the FFT analysis at low and
mid intensities. **B**: Changes in threshold. Increase in threshold relative to the unmasked
condition for varying intensities of the masker. The lock-in threshold was less affected by
the noise than the FFT analysis at each noise level.

Figure 5.
Surgical site pictures, threshold determinations, and recordings of cochlear response during penetrating wire insertion as measured from three extracochlear sites. Surgical exposures of the cochlea for each site are shown in the left most panels. The stapedial artery can be seen coursing adjacent to the round window niche. The penetrating wire (arrow) can be seen going through the RW with a radial trajectory aiming for the BM. The recording electrode (arrowhead) is placed against a bony surface of the cochlea at appropriate extracochlear sites. The middle panels display FFT (solid black circles) and lock-in (open red circles) threshold measurements at each of the extracochlear recording sites. The right panels show change in cochlear response to a 4 kHz stimulus at 70 dB SPL with intracochlear wire

insertion. The abscissa represents penetration depth (μm) and the ordinate gives response magnitude relative to that with the penetration wire at the RW (dotted line at 1.0). After wire insertion and electrophysiological evidence of damage was noted (arrows), the wire was withdrawn either partially (panel C & I) or completely (panel F) to check for reversibility.
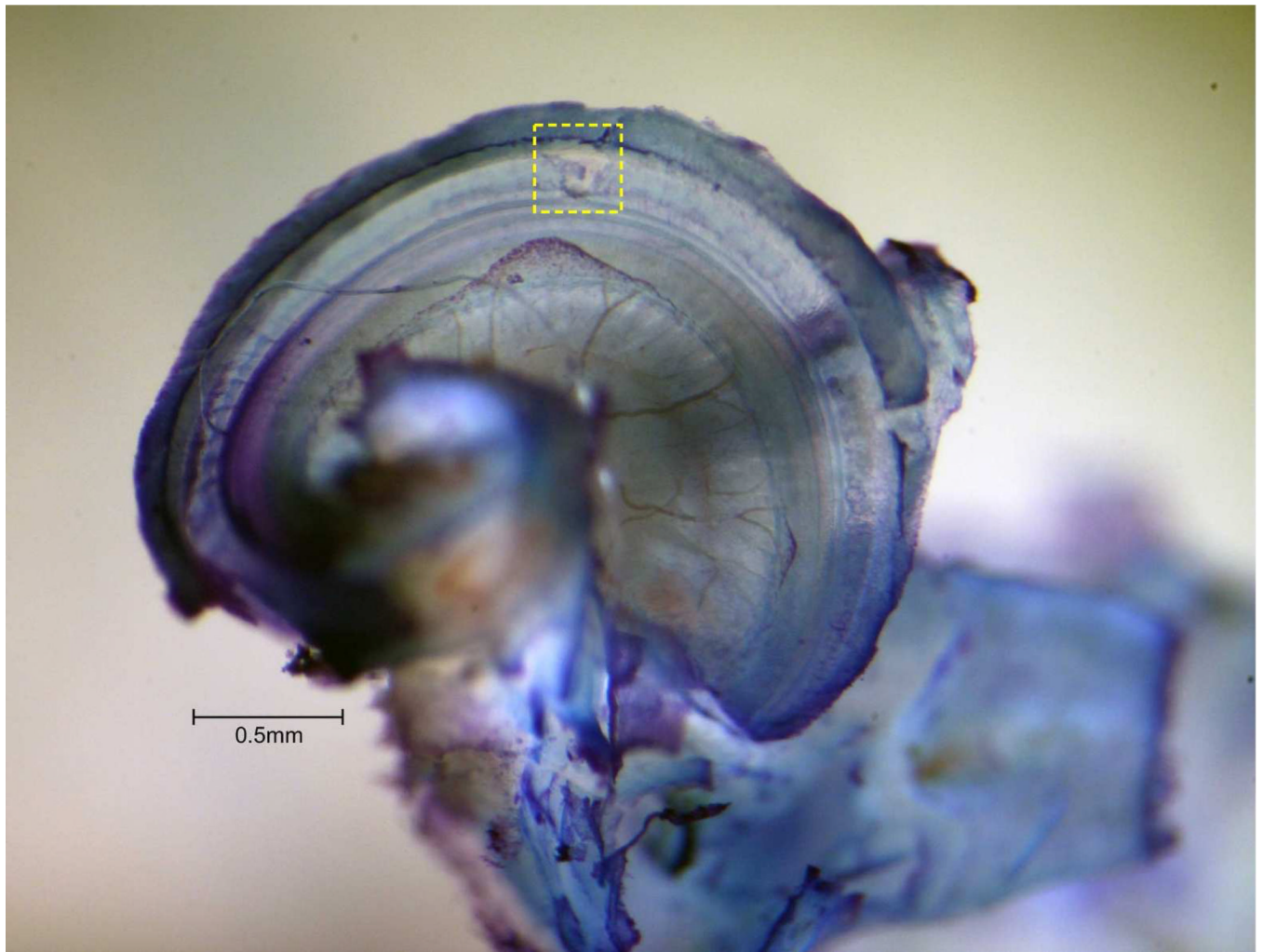
Figure 6.
Example of damage to basilar membrane cause by a radially oriented, penetrating wire insertion, as viewed from the top (scala media side, with upper turns). The preparation shown is a decalcified whole mount stained with toluidine blue. The vantage point for this image is from the apex of the cochlea but offset and the RW membrane is behind the plane of the image. Damage is outlined by the yellow hashed box and a scale is provided for reference. The physiology data in Figure 5C corresponds to this case.